Improved calibration of the ECE radiometers towards power deposition studies in W7-X

V Murugesan*[(1)], M Hirsch [(1)], G Weir [(1)], J F Guerrero Arnaiz [(1)], T Stange [(1)], M Stern [(1)], M Arvanitou [(1)], N Chaudhary [(1)], R C Wolf [(1)], and the W7-X team [(a)]

[1] *Max-Planck-Institute for Plasma Physics, Greifswald, Germany*

[a] *see O. Grulke et al 2024 Nucl. Fusion 64 112002 for a full author list*

At the optimized stellarator Wendelstein 7-X (W7-X) [1], Electron Cyclotron Emission (ECE) radiometers play an important role in deriving the core electron temperatures (T_e). At a standard magnetic field on axis $B_0 = 2.52$ T, X-mode polarized Electron Cyclotron Resonance Heating (ECRH) [2] is used as a primary heating method. The 11 ECRH gyrotrons operate at 140 GHz with powers ranging from 0.25-1 MW each. For typical plasma conditions in the plasma core at W7-X, the ECE behaves like a black body radiation from a localised layer in the plasma at the second harmonic of ECE at X mode (X2) with emission frequencies ranging from 126-162 GHz [3].
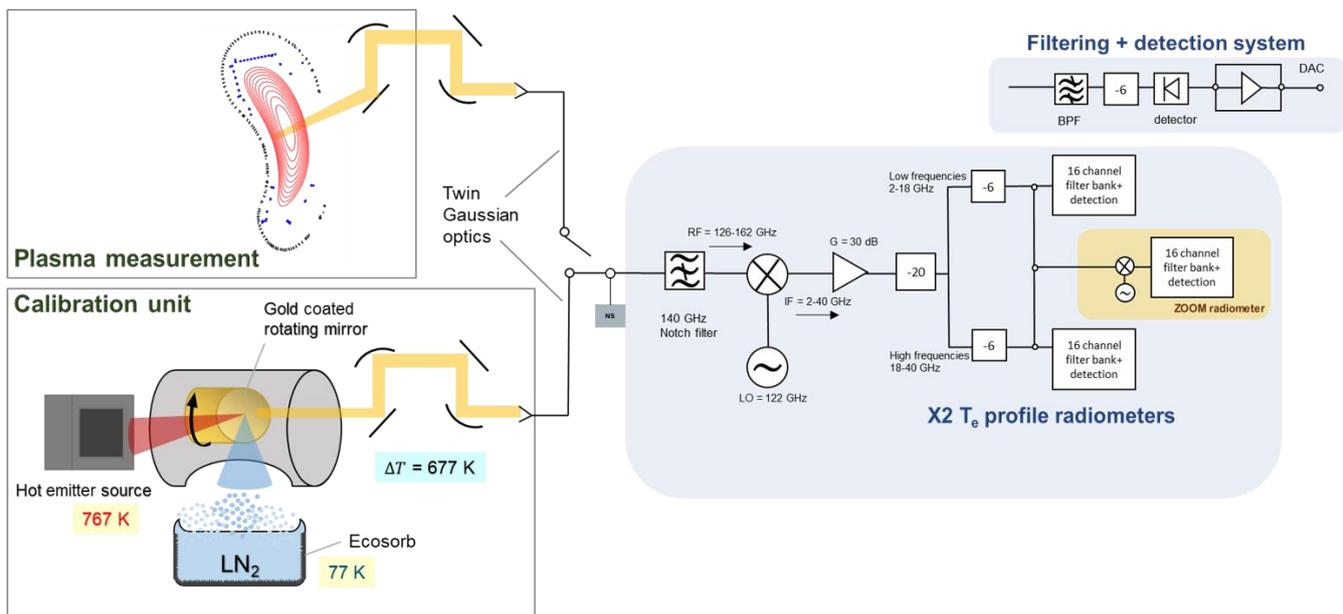

Figure 1: Schematic drawing of the ECE Hot-cold calibration unit, adapted from [4]

Standalone calibration of ECE radiometers is of special interest, as it not only results in accurate temperature profiles but also allows for the T_e data to be used in control applications. Once such application discussed here is the derived ECRH power deposition profiles.

Calibration of the ECE radiometers

There are two methods of absolute calibration followed for the ECE radiometers at W7-X:

1) "Noise source" calibration with a calibrated D-band noise source

2) "Hot cold" calibration with a temperature difference produced by blackbodies

The ***D band noise source*** (NS) can generate frequencies 110-170 GHz, fit to mimic the X2 plasma ECE. However, the installed position of this NS excludes the Gaussian optics and transmission line losses (~20 dB). In a ***Hot-cold calibration*** as shown in figure 1, liquid nitrogen (LN$_2$) in a vessel lined with Ecosorb material and a ceramic hot emitter source (HS) are used as the reference blackbody sources. The calibration sources are located in the torus hall with a twin Gaussian optics setup, so that the transmission line losses are the same as during plasma measurement. A continuously rotating mirror at a frequency of 3Hz, alternating between the sources, directs the radiation towards the radiometers. The temperature difference produced by this method of about 670 K is used as the calibration signal by the Y-method [5].
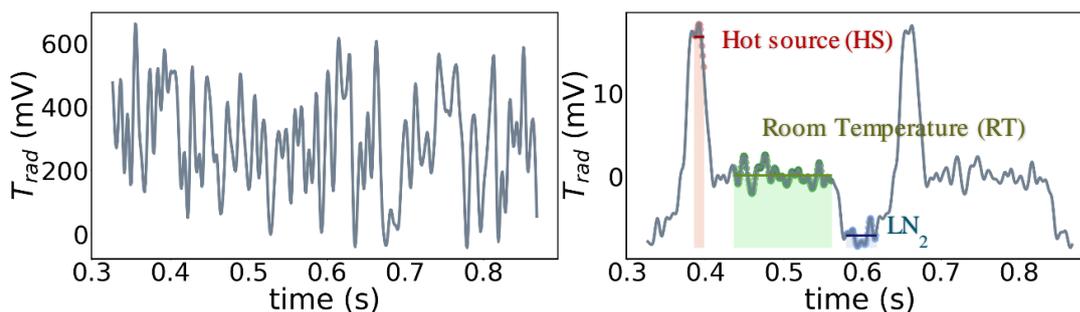
Conditional averaging for calibration

Figure 2: (Left) *unprocessed calibration signal* (Right) *After digital processing and averaging for ~ 2 hours*

The challenge in performing this Hot-Cold calibration is that the signal to noise ratio is too poor to differentiate between the hot and cold periods (figure (2-left)). An accurate measure of this difference is essential and this dU (bits) is ultimately the measure of a radiometer channel's sensitivity. The solution sought is the conditional averaging using python. A trigger signal representative of the rotating mirror (shown in figure (1)) whose frequency is digitized and stored, is used as a reference for the conditional averaging. In the final averaged signal (figure (2 (right)), the difference between the hot and cold periods can be seen well. The scatter in the averaged signal and the uncertainty in source temperatures contribute to the errors in the measured radiation temperatures. As the averaging can be done with an observation time of 1-2 hours, this proves to be a fast and effective calibration method.

The linearity of the radiometers can be verified to some extent by comparing the response

'dU' to the three available temperature differences 'dT', namely between T_{room}-T_{LN2}, T_{room}-T_{HS}, T_{LN2}-T_{HS}. Although the slope of this linearity looks different for every radiometer channel, being a measure of its sensitivity, we can see that the response is largely linear.
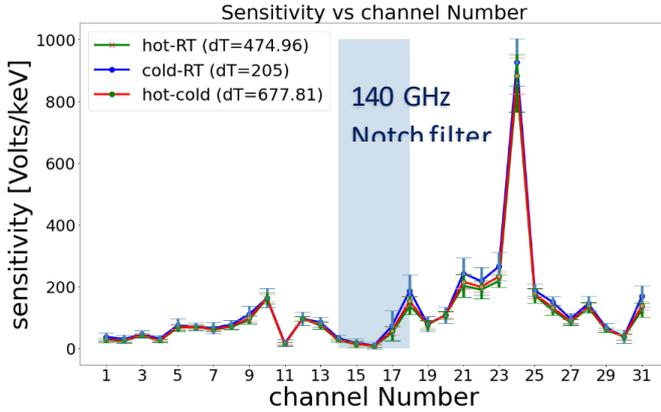

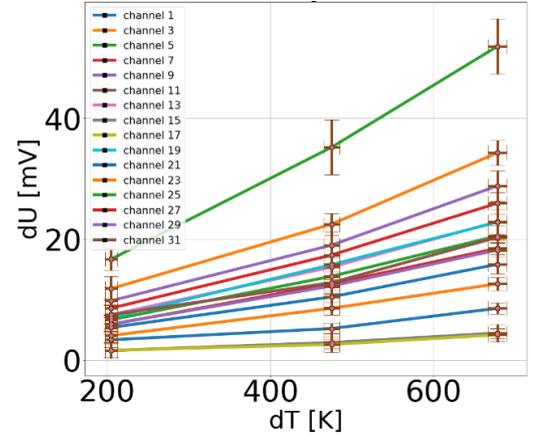*Figure 3: The sensitivity of the radiometer system measured with different calibration sources*

Figure 4: Linearity of channels

ECRH power deposition profiles during modulations

ECRH power steps and power modulations are effective experimental methods of measuring the ECRH power deposition profile [6]. Standalone calibrated ECE radiometers offer the possibility of quantifying the amount of power deposit.
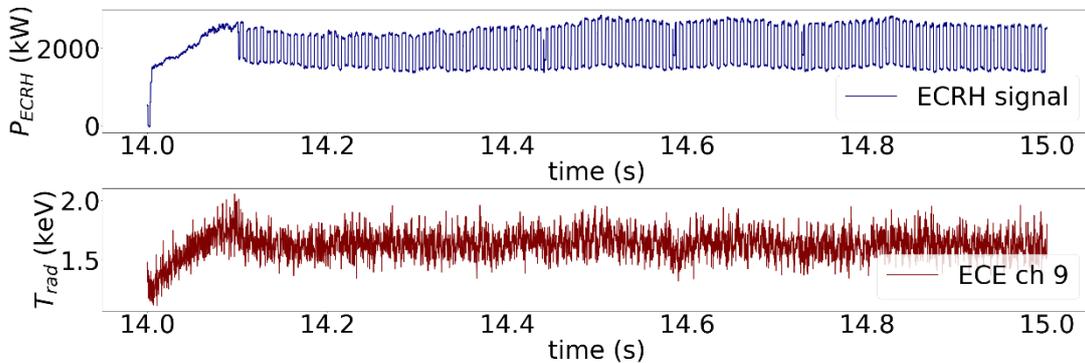

Figure 5: XP: 20250508.32

(Top) ECRH total power – f_{mod} 133 Hz (Bottom) ECE channel response to the modulation

During high frequency modulations of ECRH, the ECE at the zone of power deposition respond to this change instantaneously [7]. This change can be seen in the Fourier space of the auto-correlated power spectrum P_{yy} of the ECE channels, at the modulation frequency (f_{mod}). At the lack of calibration, the power deposition profile shapes can be observed using the mean squared-coherence "C_{xy}" between the ECRH and ECE signals. A high frequency resolution 'ZOOM' system, whose measurement position is selected by changing the local oscillator (LO) input, is used to gain high resolution in the zone of power deposition. A high-resolution

scan of the deposition zone is performed around the deposition zone by keeping other plasma parameters constant and moving the position of the ZOOM system.
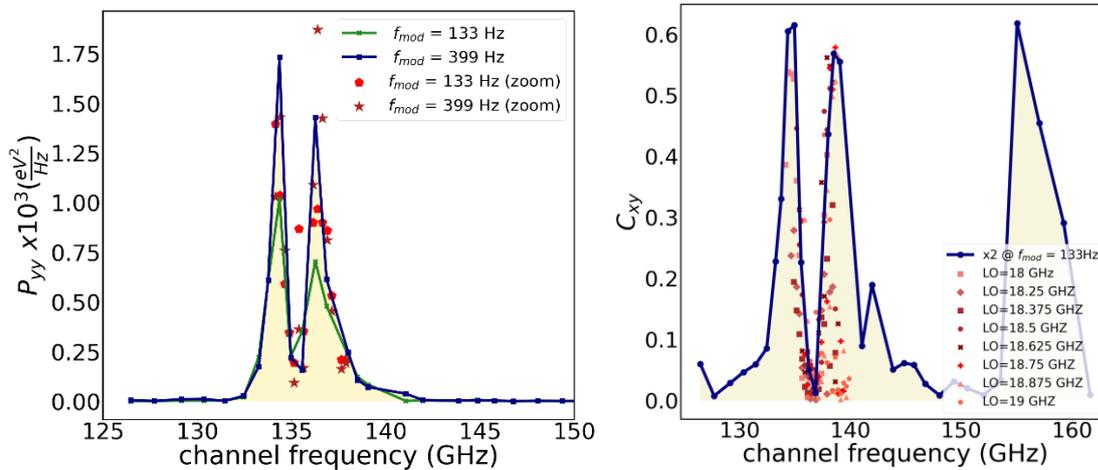

Figure 6: ECRH power deposition profiles-X2 heating, B_0=2.52 T

(Left): XP20250408.32 – ON-axis heating, (Right): XP20250522.60 to 74 – Off-axis heating

The obtained power deposition profiles are found to be narrow and symmetric around the magnetic axis for nominal "on-axis", X2 ECR heating. For off-axis heating, a third peak is observed at the high field side. Following studies will be focussed on quantifying the power deposit and deriving the deposition profiles for variety of W7-X heating conditions such as O2 heating.

Acknowledgement

References

1) *Klinger, Thomas, et al. Nuclear Fusion 59.11 (2019): 112004*

2) *Laqua, H. P., et al. Nuclear Fusion 61.10 (2021): 106005*

3) *Hirsch, M., et al., EPJ Web of Conferences, vol. 203, p. 03007, EDP Sciences, 2019*

4) *Hoefel, U., et al., Review of Scientific Instruments 90.4 (2019)*

5) *Hartfuss, H. J., & Geist, T. (2013) John Wiley & Sons*

6) *Eguilior, S., et al., Plasma physics and controlled fusion 45.2 (2003): 105*

7) *Van Eester, D., Plasma physics and controlled fusion, 46(11), p. 1675, 2004*